Atmos. Meas. Tech., 9, 1025–1037, 2016
www.atmos-meas-tech.net/9/1025/2016/
doi:10.5194/amt-9-1025-2016

Atmospheric Measurement Techniques
Open Access
EGU

Size distribution of particle-associated polybrominated diphenyl ethers (PBDEs) and their implications for health

Yan Lyu[1], Tingting Xu[1], Xiang Li[1], Tiantao Cheng[1], Xin Yang[1], Xiaomin Sun[2], and Jianmin Chen[1]

[1]Shanghai Key Laboratory of Atmospheric Particle Pollution and Prevention (LAP3), Department of Environmental Science & Engineering, Fudan University, Shanghai 200032, China
[2]Environment Research Institute, Shandong University, Jinan 250100, China

Correspondence to: Xiang Li (lixiang@fudan.edu.cn) and Xiaomin Sun (sxmwch@sdu.edu.cn)

Received: 19 October 2015 – Published in Atmos. Meas. Tech. Discuss.: 9 December 2015
Revised: 1 March 2016 – Accepted: 3 March 2016 – Published: 14 March 2016

Abstract. In order to better understand the size distribution of particle-associated PBDEs and their deposition pattern in the human respiratory tract, we carried out a 1-year campaign during 2012–2013 for the measurement of size-resolved particles at the urban site of Shanghai. The results showed that particulate PBDEs exhibited a bimodal distribution with a mode peak in the accumulation particle size range and the second mode peak in the coarse particle size ranges. As the number of bromine atoms in the molecule increases, accumulation-mode peak intensity increased while coarse-mode peak intensity decreased. This change was consistent with the variation of PBDEs' subcooled vapor pressure. Absorption and adsorption processes dominated the distribution of PBDEs among the different size particles. The evaluated deposition flux of Σ13 PBDEs was 26.8 pg h^{-1}, in which coarse particles contributed most PBDEs in head and tracheobronchial regions, while fine-mode particles contributed major PBDEs in the alveoli region. In association with the fact that fine particles can penetrate deeper into the respiratory system, fine-particle-bound highly brominated PBDEs can be inhaled more deeply into human lungs and cause a greater risk to human health.

1 Introduction

Polybrominated diphenyl ethers (PBDEs) are a class of organobromine compounds that are widely used as a flame retardant. They are applied to a broad array of textiles and consumer products including plastics, polymers, mattresses, upholstery, carpeting, building materials and electronic equipment (de Wit, 2002; Alaee et al., 2003). Because the compounds are additive rather than chemically bound to the products, they can be released into the environment. They are persistent organic chemicals and can bioaccumulate, therefore, they have become contaminants detectable in the environment, in animals and in humans (Su et al., 2009; Besis and Samara, 2012). Human uptake is thought to be through inhalation, dermal absorption and consumption of contaminated food (Marklund et al., 2003; Wensing et al., 2005). The primary source of exposure to humans is believed to be consumption of contaminated fish, poultry, meat and dairy products (Su et al., 2009; Besis and Samara, 2012). Occupational exposures may occur in computer, electronic warehouses and formulation facilities (Harrad et al., 2010). Inhalation exposure can take place through ambient aerosol or dust containing PBDEs. Compared with dust PBDEs, the inhalation of ambient aerosols may be a minor pathway for humans, but it has a long-term bioaccumulation process in the human body. When PBDEs are suspended in air, they can be present as particles. Since we can not say how long PBDEs remain in the air, long-term exposure to PBDEs has a greater potential to cause health effects than does short-term exposure to low levels because of their tendency to build up in the human body over many years. Growing concerns about the health impacts of PBDEs have led to a decline in their production and finally, a ban of their use in the United States and Europe since 2004 (Kemmlein et al., 2009). All technical mixtures of PBDEs were also totally phased out in other regions, including China (Betts, 2008). However, it is likely that long-term exposure will continue long after PBDE production has ended through emissions from PBDE-containing

products that are still being used. Thus, it has become necessary to investigate the characteristics of particulate PBDEs existing in urban ambient aerosols.

Over the past decade, measurements of atmospheric PBDEs have been carried out in various areas around the world, such as Turkey (Cetin and Odabasi, 2008), Japan (Kakimoto et al., 2014), Thailand (Muenhor et al., 2010) and China (Yang et al., 2013) in Asia; the United States (Hale et al., 2003) and Canada (Wilford et al., 2004) in North America; Greece (Besis et al., 2015), France (Castro-Jimenez et al., 2011) and the Czech Republic (Okonski et al., 2014) in Europe; and some places in the Arctic (Moller et al., 2011; Wang et al., 2005). In these studies, particulate PBDEs were mainly investigated in individual particle size fractions such as $PM_{2.5}$ and PM_{10}, and were rarely related with size-resolved particles. Size distribution of particle-associated PBDEs is crucial when evaluating human health risks since the size-resolved particles dominate the deposition behavior of particles in the respiratory tract. To the best of our knowledge, particle size distribution of PBDEs was merely reported in Thessaloniki, Athens (Greece) (Mandalakis et al., 2009; Besis et al., 2015), at e-waste recycling sites close to Guangzhou (China) (B. Z. Zhang et al., 2012; Luo et al., 2014b) and at Brno (Czech Republic) (Okonski et al., 2014). These studies showed that major lighter brominated congeners existed on coarse particles, while most highly brominated congeners occurred on fine particles. In association with the fact that fine particles can easily penetrate/enter the alveolar region, fine-particle-bound highly brominated congeners can travel deep into the lungs and cause serious health problems for humans (Geiser et al., 2005). To clarify this issue we first need to investigate the actual particle size distribution of PBDEs through long-term observations.

This investigation was conducted in the urban site of Shanghai with the aim of evaluating the size distribution of particle-associated PBDEs and their deposition in the human respiratory tract. Besides this, the elucidation of the influence of some factors such as the volatility, the chemical affinities and releasing source on these distributions was also attempted.

2 Experimental and methods

2.1 Chemicals

Standard mixtures of PBDEs (BDE-17, 28, 47, 66, 71, 85, 99, 100, 138, 153, 154, 183, 190 and 209) were purchased from AccuStandard, Inc. (United States). Internal standards (^{13}C-BDE-28, 47, 99 and 153) were purchased from Cambridge Isotope Laboratories (Andover, MA). PBDE congeners were divided into five groups (e.g., tri-, tetra-, penta-, hexa- and hepta-BDE) based on the number of bromine atoms in the molecule. The solvents used in this research were high-performance liquid chromatography (HPLC)/spectro grade and bought from Tedia Company Inc. (United States).

2.2 Sample collection

The sampling campaign took place on the rooftop (20 m above the ground) of teaching building No. 4 at Fudan University campus (121.50° E, 31.30° N), approximately 5 km northeast of downtown Shanghai (elevation about 4 m a.s.l.). A Fudan super monitoring station for atmospheric chemistry was running here all year round. The site is in close proximity to shopping malls and residences, and the traffic around is busy due to the close proximity to the sub-downtown. The main PBDE-releasing sources at this site included industries emission, household heating and road transport. Details regarding the sampling site are included in our previous work (P. F. Li et al., 2011; X. Li et al., 2011). Particle samples were collected by drawing air through a quartz fiber filter (Whatman QMA, ∅81 mm), using an Anderson 8-stage air sampler (Tisch Environmental Inc., United States). The flow rate was controlled at 28.3 L min^{-1}. The cutoff aerodynamic diameters for each stage were < 0.4, 0.4–0.7, 0.7–1.1, 1.1–2.1, 2.1–3.3, 3.3–4.7, 4.7–5.8, 5.8–9.0 and > 9.0 µm. The whole measurement period ranged from December 2012 to November 2013. The sampling time was 120 h for each sample batch. A total of 189 particle samples (21 sample batches containing 9 size fractions) were obtained at this site. Prior to sampling, the filters that were wrapped in aluminum foil were baked at 450 °C for 12 h to remove organic materials. After sampling, loaded filters, together with aluminum foils, were stored at −20 °C until extraction. In addition, meteorological data during the measurement period were obtained from the Fudan atmospheric monitoring station (Lv et al., 2015).

2.3 Sample extraction

The aerosol samples were extracted by a Soxhlet extractor with a mixture of dichloromethane/hexane (1 : 1, v/v). The extraction time was 36 h at a constant temperature of 69°C. After extraction, the samples were filtered through 0.45 µm PTFE syringe filters and concentrated using a rotary evaporator (BÜCHI Rotavapor®, Switzerland) and a pure N_2 stream.

2.4 Instrumental analysis

Each compound was quantified by an Agilent 7890A Series gas chromatograph (GC) coupled to an Agilent 7000B Triple Quadruple Mass Spectrometer (GC/MS/MS, Agilent Technologies Inc., United States) operating at electron impact energy of 70 ev and using the multiple reaction monitoring mode. Samples' separation was carried out by a DB-5ms (15 m × 0.25 mm inner diameter with 0.25 µm film thickness) capillary column (J&W Scientific, Folsom, CA). The column temperature was initially at 150 °C, then proceeded to increase from 12 °C min^{-1} to 315 °C with 2 min hold. All samples were automatically injected with 2 µL in pulse split-

less mode. The injector temperature was set to 330 °C, the transfer line to 310 °C and the ion trap to 300 °C. High-purity helium (99.999 %) was applied as a carrier gas with a constant flow rate of 1.2 mL min^{-1} in the column. Nitrogen gas was used as the collision gas in the MS. The identification and quantification of PBDEs were done according to retention times, selected precursor ions, product ions and the internal standard method relative to the closest eluting PBDE surrogate. The calibration solutions were prepared at five concentrations and contained uniform concentrations of the internal standards. For each analyte, a relative response factor was determined for each calibration level using the internal standard. The five response factors were then averaged to produce a mean relative response factor for each species. Reported analyte concentrations were corrected for internal standards recoveries. The calibration curves showed a linear response in the range 0.1–5 µg L^{-1}. The correlation coefficients of the calibration curve for the different PBDEs were $R^2 > 0.99$.

2.5 Quality control and assurance

Each batch of samples included one procedural blank. In that case, only BDE-71, 100, 154 and 190 were commonly detected at much lower levels (< 5 %) in some samples. The mean values of blanks were then subtracted from measured values of each sample. Method recoveries determined by spiking the sampling process (five replicates) with a standard mixture of PBDEs ranged from 75 to 175 %. In addition, isotopically labeled PBDEs were added as an internal standard (added after extraction and clean-up, just prior to GC-MS analysis) to check the instrument performance. Recoveries were between 90 and 110 %. As a further quality control step, SRM 2585 (NIST, Gaithersburg, MD, United States) was used as the reference material in this study. Measured PBDE levels in SRM 2585 ranged from 75 to 120 % of certified values. Repeatability was evaluated by performing four analyses of a standard PBDEs solution containing the above-mentioned PBDEs and the surrogate standards in the same conditions. The relative standard deviations of the relative response factors were below 10 % for all PBDEs. The method detection limits (DLs) and quantification limits were calculated as the concentrations equivalent to 3 and 10 times the noise of the quantifier ion for a blank sample (the DL ranged from 0.05 to 0.6 pg m^{-3}). For the purpose of statistical analysis, samples with concentrations under limit of detection (LOD) were assigned concentrations equal to 0.5 LOD (Okonski et al., 2014).

2.6 Size-specific gas/particle partition

Two processes are commonly accepted for illustrating mechanisms of particle–gas partition, i.e., adsorption and absorption process. In the case of adsorption, it assumes that chemicals adsorb to active sites on the surface of the particle. The gas–particle partitioning coefficients ($K_{\text{p-ads}}$) during the adsorption process are described by Pankow (1987):

$$K_{\text{p-ads}} = \frac{N_{\text{s}} A_{\text{TSP}} T e^{(Q_{\text{L}} - Q_{\text{v}})/RT}}{1600 p_{\text{L}}^{\circ}}, \quad (1)$$

where N_{s} is the surface concentration of sorption sites (4×10^{-10} mol cm^{-2}), A_{TSP} is the specific surface area of the particles, T is the ambient temperature (292 K), R is the ideal gas constant (8.31 J mol^{-1} K^{-1}), Q_{L} and Q_{v} are the enthalpy of desorption from the surface and the enthalpy of vaporization of the subcooled liquid (kJ mol^{-1}), respectively and p_{L}° is the vapor pressure of the subcooled liquid. In contrast with PAHs, a similar situation was assumed for PBDEs that $Q_{\text{L}} - Q_{\text{v}} \approx 1 \times 10^4$ J mol^{-1} (Aubin and Abbatt, 2006). After logarithmic transformation on both sides in Eq. (1), we obtain Eq. (2) as follows:

$$\log K_{\text{p-ads}} = -\log p_{\text{L}}^{\circ} + \log A_{\text{TSP}} - 8.35. \quad (2)$$

Size-dependent A_{TSP} adopted from the results of Yu and Yu (2012) and the data are listed in Table 2. Based on three modes, we then obtained Eq. (3) which is derived from Eq. (2).

$$\log K_{\text{p-ads}} = \quad (3)$$

$$\begin{cases} -\log p_{\text{L}}^{\circ} - 6.64 & \text{(Aitken mode: } < 0.4\,\mu\text{m)} \\ -\log p_{\text{L}}^{\circ} - 7.25 & \text{(Accumulation mode: } 0.4 - 2.1\,\mu\text{m)} \\ -\log p_{\text{L}}^{\circ} - 7.06 & \text{(Coarse mode: } 2.1 - 10\,\mu\text{m)} \end{cases}$$

The temperature-dependent p_{L}° values of PBDE congeners were calculated using the regression parameters by ($\log p_{\text{L}}^{\circ} = A + B/T$) (Tittlemier et al., 2002). In our study, the average temperature of the sampling campaign was 292 K. The temperature-dependent p_{L}° is listed in Table 1.

In the case of absorption, it assumes that atmospheric aerosols are coated with an organic film and chemicals can absorb into this organic phase. The gas–particle partitioning coefficients ($K_{\text{p-abs}}$) during the absorption process are described by Finizio et al. (1997):

$$K_{\text{p-abs}} = 10^{-9} \frac{M_{\text{o}} \gamma_{\text{o}}}{M_{\text{OM}} \gamma_{\text{OM}} \rho_{\text{OM}}} f_{\text{OM}} K_{\text{OA}}, \quad (4)$$

where M_{o} and M_{OM} are the mean molecular weights of octanol and the organic matter phase (g mol^{-1}), and γ_{o} and γ_{OM} are the activity coefficients of the absorbing compound in octanol and in the organic matter phase, respectively. f_{OM} is the fraction of organic matter phase on particles; K_{OA} is the octanol–air partition coefficient. ρ_{OM} is the density of octanol (820 kg m^{-3} at 20°).

With the assumption that $\frac{M_{\text{o}}}{M_{\text{OM}}} = 1$, $\frac{\gamma_{\text{o}}}{\gamma_{\text{OM}}} = 1$, Eq. (4) can be simplified to Eq. (5) after logarithmic transformation on both sides:

$$\log K_{\text{p-abs}} = \log K_{\text{OA}} + \log f_{\text{OM}} - 11.91. \quad (5)$$

Table 1. Physiochemical properties reference dose (RfD) of the target PBDE congeners and data from Yang et al. (2013).

Chemical	Molecule	MW[a]	RfD	$\log p_L^\circ/(p_a)$[b]	$\log K_{OA}^c$	Gas phase[e] ($pg\,m^{-3}$)	Particulate phase[e] ($pg\,m^{-3}$)
BDE-17	2,2′,4-tribromodiphenyl ether	406.9	1.0×10^5	−2.71[d]	9.31	15.64	0.93
BDE-28	2,4,4′-tribromodiphenyl ether	406.9	1.0×10^5	−2.95	9.4	30.04	1.17
BDE-71	2,3′,4′,6-tetrabromodiphenyl ether	485.8	1.0×10^5	−3.55[d]	10.2	–	–
BDE-47	2,2′,4,4′-tetrabromodiphenyl ether	485.8	1.0×10^5	−4.07	10.1	28.81	5.38
BDE-66	2,3′,4,4′-tetrabromodiphenyl ether	485.8	1.0×10^5	−4.27	10.25	6.11	0.38
BDE-100	2,2′,4,4′,6-pentabromodiphenyl ether	564.7	1.0×10^5	−4.91	10.82	3.38	1.52
BDE-99	2,2′,4,4′,5-pentabromodiphenyl ether	564.7	1.0×10^5	−5.14	10.96	8.02	5.06
BDE-85	2,2′,3,4,4′-pentabromodiphenyl ether	564.7	1.0×10^5	−5.40	11.03	2.58	2.42
BDE-154	2,2′,4,4′,5,6′-hexabromodiphenyl ether	643.6	2.0×10^5	−5.83	11.66	1.37	2.10
BDE-153	2,2′,4,4′,5,5′-hexabromodiphenyl ether	643.6	2.0×10^5	−6.08	11.77	1.27	2.39
BDE-138	2,2′,3,4,4′,5′-hexabromodiphenyl ether	643.6	2.0×10^5	−6.23	11.81	1.09	2.21
BDE-183	2,2′,3,4,4′,5′,6-heptabromodiphenyl ether	722.5	2.0×10^5	−6.75	12.52	1.67	10.01
BDE-190	2,3,3′,4,4′,5,6-heptabromodiphenyl ether	722.5	2.0×10^5	−7.00	12.71	–	–

[a] Molecular weight. [b] Subcooled liquid vapor pressure in 292 K from Tittlemier et al. (2002). [c] Octanol–air partition coefficient in 292 K from Harner and Shoeib (1998); [d] data from Wang et al. (2008). [e] Data from Yang et al. (2013). [f] Oral reference doses ($pg\,kg^{-1}\,bw\,day^{-1}$) of BDE-47, 99, 153 were suggested by the US Environmental Protection Agency's IRIS database (www.epa.gov/iris) and RfDs of other tetra-, penta-, hexa-BDE congeners were assumed to be equivalent reference doses of BDE congeners with the same bromine atoms. In addition, RfDs of tri-BDE and hepta-BDE were assumed to be the same as those of BDE-47 and BDE-153, respectively.

Table 2. A_{TSP} and f_{OM} adopted from Yu and Yu (2012).

μm	< 0.4	0.4–0.7	0.7–1.1	1.1–2.1	2.1–3.3	3.3–4.7	4.7–5.8	5.8–9	9–10
A_{TSP} ($m^2\,g^{-1}$)	50	10	10	19	19	19	19	19	19
f_{OM}	0.45	0.35	0.35	0.25	0.25	0.25	0.25	0.25	0.25

Size-specific f_{OM} was adopted from Yu and Yu (2012) and is listed in Table 2. Through calculation, we can deduce Eq. (6) as follows:

$$\log K_{\text{p-abs}} = \begin{cases} \log K_{OA} - 12.26 & \text{(Aitken mode: } < 0.4\,\mu\text{m)} \\ \log K_{OA} - 12.42 & \text{(Accumulation mode: } 0.4 - 2.1\,\mu\text{m)} \\ \log K_{OA} - 12.51 & \text{(Coarse mode: } 2.1 - 10\,\mu\text{m)}. \end{cases} \quad (6)$$

K_{OA} has been reported as a function of temperature ($\log K_{OA} = A + B/T$) (Harner and Shoeib, 2002). In this study, the average temperature of the sampling campaign was 292 K. The temperature-dependent $\log K_{OA}$ is listed in Table 1, along with other physiochemical properties of the target PBDE congeners.

Pankow (1994a) proposed a definition of the measured particle–gas partition coefficient ($K_{\text{p-measured}}$) to characterize the partitioning behavior of semi-volatile organic compounds (SVOCs) between the gas and particulate phases:

$$K_{\text{p-measured}} = (P/\text{TSP})/G, \quad (7)$$

where P and G are PBDEs in particulate- and gas-phase concentration, respectively, and TSP is the total suspended particulate ($\mu g\,m^{-3}$). After linear regression between $\log K_{\text{p-measured}} \sim \log p_L^\circ$ and $\log K_{\text{p-measured}} \sim \log K_{OA}$, we can obtain the relationship between $\log K_{\text{p-measured}} \sim \log p_L^\circ$ and $K_{\text{p-measured}} \sim \log K_{OA}$.

In association with Eqs. (4), (6) and (7), we can investigate the sorption mechanisms governing particle size distribution of PBDEs by comparing theoretical $K_{\text{p-ads}}$ and $K_{\text{p-abs}}$ with measured $K_{\text{p-measured}}$.

2.7 Human respiratory risk assessment

Because the size-resolved particles played a key role in health risk assessment through inhalation (Luo et al., 2014a), we adopted a so-called International Commission on Radiological Protection (ICRP) model (1995) to evaluate the deposition efficiencies and fluxes of inhaled PBDEs in the human respiratory tract. The human respiratory tract can be divided into three regions: head airway (HA), tracheobronchial region (TB), and alveoli region (AR). The particle deposition efficiency (DE) in HA, TB and AR is estimated by the followed simplified Eqs. (8)–(10):

$$\text{DE}_{\text{HA}} = \text{IF} \times \left[\frac{1}{1 + e^{6.84 + 1.183 \ln D_p}} + \frac{1}{1 + e^{0.924 - 1.885 \ln D_p}} \right] \quad (8)$$

Table 3. Seasonal concentrations of size-resolved particulate PBDEs in the urban site of Shanghai (pg m^{-3}).

Compound	Spring		Summer		Autumn		Winter	
	Mean	Range	Mean	Range	Mean	Range	Mean	Range
BDE-17	nd	nd–0.37	0.08	nd–0.27	0.11	nd–0.52	0.10	nd–0.46
BDE-28	nd	nd–0.18	nd	nd–0.13	nd	nd–0.18	0.11	nd–0.68
BDE-71	nd	nd–0.17	nd	nd–0.18	nd	nd–0.19	nd	nd–0.93
BDE-47	0.48	0.24–0.82	0.57	0.35–1.12	0.44	0.24–0.80	0.38	0.11–1.16
BDE-66	nd	nd–0.16	nd	nd–0.19	nd	nd	0.16	nd–1.46
BDE-100	nd	nd	nd	nd	nd	nd	nd	nd–0.23
BDE-99	3.28	1.27–6.73	1.74	1.01–7.10	4.14	0.63–8.29	4.74	1.61–12.4
BDE-85	2.38	0.78–7.15	1.12	0.31–3.06	2.31	0.45–4.50	3.54	0.81–12.2
BDE-154	nd	nd–2.85	nd	nd–0.42	nd	nd	nd	nd–2.85
BDE-153	1.08	nd–3.07	0.44	nd–2.40	0.42	nd–2.15	1.29	nd–5.43
BDE-138	1.05	0.30–2.85	0.46	nd–2.19	1.20	0.34–2.15	1.18	0.29–2.89
BDE-183	0.65	nd–0.78	nd	nd–0.67	0.72	nd–1.12	0.81	nd–1.25
BDE-190	nd	nd–0.91	nd	nd	nd	nd–0.76	nd	nd–0.96
Σ_{13}PBDE	90.3	76.3–106	52.6	30.6–82.2	93.9	90.7–100	117	104–141

nd denotes values that are not detected.

$$\mathrm{DE_{TB}} = \left(\frac{3.52\times10^{-3}}{D_\mathrm{p}}\right) \times \left[e^{-0.234(\ln D_\mathrm{p}+3.40)^2} + 63.9\times e^{-0.819(\ln D_\mathrm{p}-1.61)^2}\right] \quad (9)$$

$$\mathrm{DE_{AR}} = \left(\frac{0.0155}{D_\mathrm{p}}\right) \times \left[e^{-0.416(\ln D_\mathrm{p}+2.84)^2} + 19.11\times e^{-0.482\left(\ln D_\mathrm{p}-1.362\right)^2}\right], \quad (10)$$

where D_p is diameter of the particle, and IF is the inhalable fraction of all particles, $\mathrm{IF} = 1-\left(1-\frac{1}{1+7.6{D_\mathrm{p}}^{2.8}\times10^{-4}}\right)/2$.

The deposition flux (DF, pg h^{-1}) of inhaled particulate PBDEs in the respiratory tract is estimated by

$$\mathrm{DF} = \sum(\mathrm{DE}_i \times C_i) \times V, \quad (11)$$

where DE_i is the particle deposition efficiency in each region for D_{p_i} (the average diameter of each particle size fraction); C_i is the PBDEs' concentration in particle D_{p_i} (pg m^{-3}); and V is the breathing rate. The lower and upper limit diameters of particles in this research were assumed to be 0.1 and 30 µm, respectively. The respiration rate under normal conditions was considered to be 0.45 m^3 h^{-1} (K. Zhang et al., 2012).

In addition, we applied hazard quotient (HQ) values to assess the non-cancer risk of size-resolved PBDEs through inhalation. The formula is as follows:

$$\mathrm{HQ} = \mathrm{DI}/(\mathrm{BW}\times\mathrm{RfD}), \quad (12)$$

where DI is daily intake (pg day^{-1}) and calculated by multiplying deposition flux (DF: pg h^{-1}) with average exposure time (ET: h day^{-1}), BW is the mean body weight of an adult (60 kg) and RfD is the reported oral reference dose for PBDEs (pg kg^{-1} bw day^{-1}).

In order to understand the impact of risk and uncertainty in size-resolved particles, we used Monte Carlo simulations to produce probability distributions of hazard levels with 5000 trials. Moreover, we used the SPSS version 22.0 (IBM company, Chicago, IL, United States) to perform Pearson correlation analysis for all data and considered p values of smaller than 0.01 or 0.05 statistically significant.

3 Results and discussion

3.1 PBDEs occurrence and seasonal variation

Most PBDE congeners were detected in the vast majority of samples (Fig. 1 and Table 3). BDE-71, 100, 154 and 190 were sometimes present close to the detection limits of the method. Due to the erratic concentration of BDE 209, this compound has been removed from further analysis. The box plot in Fig. 1 summarizes the concentrations measured throughout the year and allows for easy visualization of PBDE congener groups (e.g., tri-, tetra-, penta-, hexa- and hepta-BDEs). The box contains the middle 50 % of the data, whereas the top and bottom end of the box represent the 75th and 25th percentiles of the data set, respectively. The extensions (whiskers) at either end of the box indicate the 95th and 5th percentile, and the solid spheres represent the maximum and minimum values. The median concentrations are indicated by the solid vertical lines, whereas the mean concentrations are depicted by the horizontal line. In general, the size of the box and the length of the whiskers are an indicator of the variability in concentrations at a given site for a given compound containing the same number of bromine

atoms. A small box shows that the distribution is uniform over the entire sampling period and vice versa. In these groups, penta-BDEs ($49.5 \pm 21.5\,pg\,m^{-3}$) were the dominant congeners detected in all samples, followed by hexa-BDE ($16.7 \pm 7.8\,pg\,m^{-3}$), hepta-BDE ($11.2 \pm 3.1\,pg\,m^{-3}$), tetra-BDE ($5.9 \pm 1.3\,pg\,m^{-3}$) and tri-BDE ($1.3 \pm 0.3\,pg\,m^{-3}$). Among individual PBDEs, PBDE-47, 99 and 85 were detected in 100 % of the ambient aerosol samples, with BDE-99 and 85 being the most dominant congeners. This may be due to the fact that less brominated BDEs have longer half-lives (years) and could be formed through debromination of more brominated congeners (Bezares-Cruz et al., 2004). The observed average concentrations of particulate Σ13 PBDEs ranged from 30.6 to 141.2 pg m^{-3}, with a mean value of 86.3 pg m^{-3} (Table 3). This result was consistent with the results of the previous measurements in Shanghai, 108–367 pg m^{-3} (Yang et al., 2013), and $104 \pm 54\,pg\,m^{-3}$ (Yu et al., 2011), but was much lower than in Beijing, 760 pg m^{-3} (Yang et al., 2013), and in waste recycling zones of Qingyuan close to Guangzhou, 3260 pg m^{-3} (Tian et al., 2011). In addition, these results were compared with those reported in aerosol samples from Ontario (Larsen and Baker, 2003), Chicago (Hoh and Hites, 2005) and three different stations in western Europe (Lee et al., 2004), as well as other Asian cities such as Osaka (9.9–22.3 pg m^{-3}) (Kakimoto et al., 2014), Busan (5.3–16 pg m^{-3}; Rudich et al., 2007) and Singapore (7.5 pg m^{-3}; Shen et al., 2013). These direct comparison of PBDEs concentrations between various urban environments should be done with caution. Because of the differences existing within any urban environment, PBDE levels could be significantly affected by the location of the sampling site and its proximity to emission sources. Moreover, sampling methodology is a critical parameter affecting the comparison between the observed concentrations of PBDEs in different sites. In most published studies, collection of particulate PBDEs has been performed by using different sampling, pretreatment and instrumental analysis system devices and in some cases, underestimation of PBDE concentrations might have occurred because more volatile species were mainly in the gas phase and easily lost during membrane sampling or the storage period.

Seasonal variations were distinct at these urban sites, with significantly higher concentrations measured during winter (104–141 pg m^{-3}) and lower concentrations measured during summer (30.6–82.2 pg m^{-3}) (Table 3). Higher concentrations in winter were at least in part due to increased emissions and due to the distinctive meteorological conditions, including reduced mixing heights and lower precipitation depth for favoring the pollutants' accumulation in the atmosphere (Volckens and Leith, 2003). In addition, the adsorption of gaseous PBDEs on particles was likely to increase during winter since the partition coefficient, K_p, was inversely correlated with temperature ($r = -0.867$, $p<0.01$) (see Fig. 2). Lower concentrations in summer may have been caused by wet scavenging since some summer sampling days experienced precipitation at this site. Seasonal variations in PBDEs can also be explained by the Asian monsoon patterns. Shanghai sites are situated in a transitional zone of the northern subtropical monsoon system, where the northwesterly winter monsoon transports polluted air masses from mainland China, while the southeasterly summer monsoon transports cleaner oceanic aerosols from the oceans (Western Pacific) (Shi and Cui, 2012). Moreover, higher wind speeds appeared to be typically associated with lower concentrations of PBDEs ($r = -0.583$, $p<0.01$) (Fig. 2). Higher concentrations of PBDEs were associated with a higher $PM_{2.5}$ level ($r = 0.629$, $p<0.01$) and lower visibility ($r = -0.686$, $p<0.01$). This seasonal pattern was consistent with those

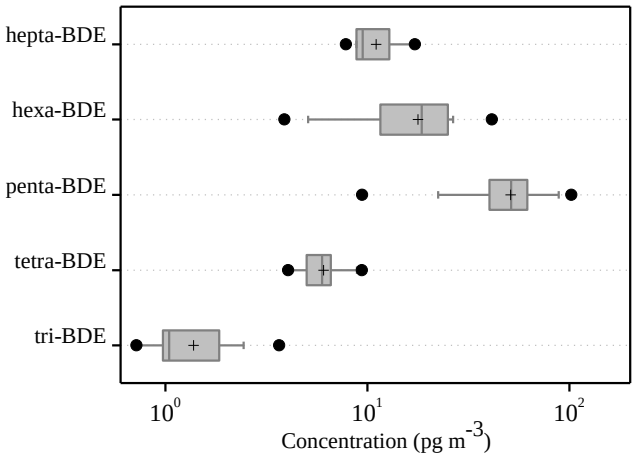

Figure 1. Concentration profiles of PBDE homologue groups in the urban atmosphere. Solid vertical lines and the horizontal lines represent median and mean values, respectively. Box plots represent 25th–75th percentiles; whiskers indicate 5th and 95th percentile. The solid circles represent maximum and minimum values.

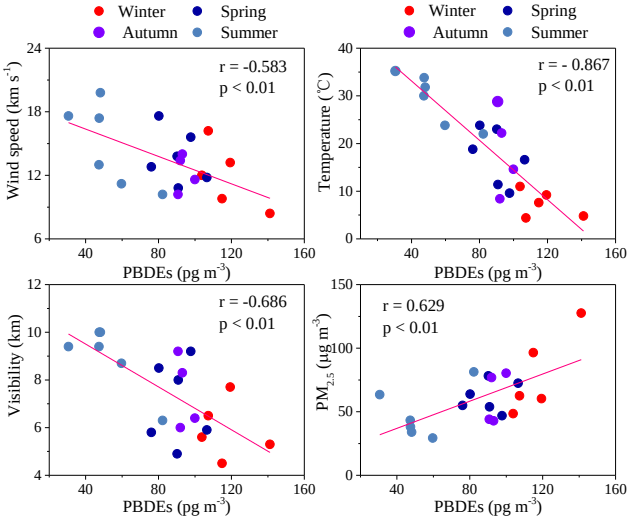

Figure 2. Pearson correlation between particulate PBDEs and weather parameters: visibility, temperature, wind speed and $PM_{2.5}$.

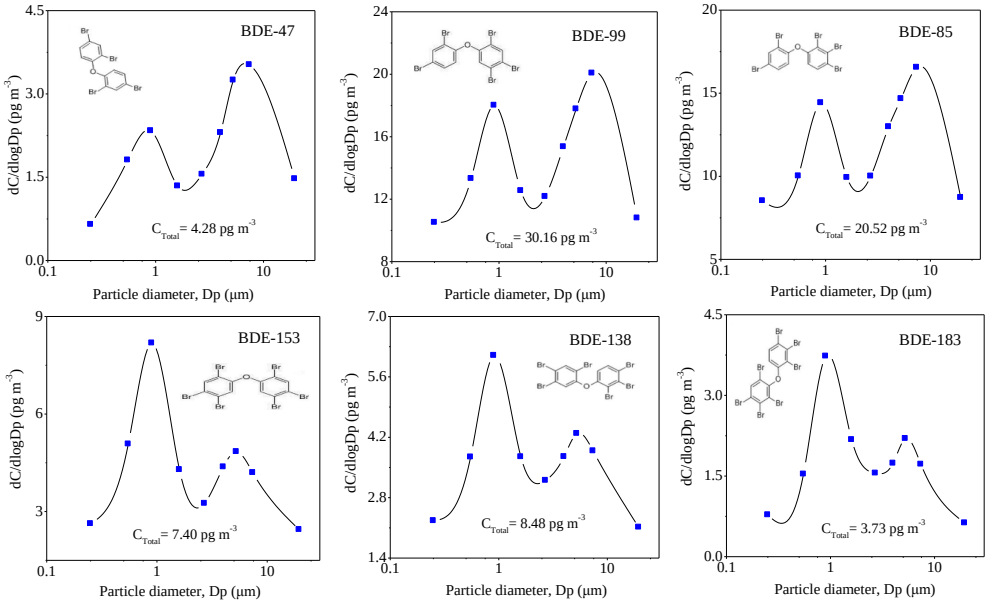

Figure 3. Mean normalized size distribution of particle-associated PBDEs for all samples. dC is the concentration on each filter, C is the sum concentration on all filters and d log D_p is the logarithmic size interval for each impactor stage in particle diameter (D_p).

measured in Huaniao Island (Li et al., 2015), Qingyuan (Tian et al., 2011) and Dongguan (Zhang et al., 2009).

3.2 Size distribution and process mechanism of particle-associated PBDEs

Among the PBDE congeners measured, we chose BDE-47, 85, 99, 138, 153 and 183 for the study of size distribution due to detection frequencies higher than other congeners. Figure 3 plots the average size distributions of these PBDEs in the continuous smoothed curves inverted from the sample data. The results showed that particulate PBDEs exhibited a bimodal distribution with a mode peak in the accumulation particle size range and the second mode peak in the coarse particle size ranges. As the number of bromine atoms in the molecule increased, accumulation-mode peak intensity increased, while coarse-mode peak intensity decreased, which indicated that the lighter brominated congeners BDE 47 and 85 were mainly associated with particles larger than 2.1 mm, whereas the highly brominated congeners were mainly sorbed to the fine particles. The similar bimodal distribution of PBDEs also occurred in Heraklion (Mandalakis et al., 2009), Brno and Telnice (Okonski et al., 2014) and Guangzhou (B. Z. Zhang et al., 2012). Differences in the particle size distribution of individual PBDEs could reflect differences in their emission sources but there was no credible scientific evidence in support of this claim. Although published data on size distribution of particle-associated PBDEs are not available for comparison, analogous trends have also been observed for other classes of organic contaminants such as PAHs. Previous field measurements by cascade impactors demonstrated that PAHs with more rings were sorbed to the fine aerosol fraction, while more volatile or species with a low number of rings were associated with larger particles (Wang et al., 2015; Kavouras et al., 1999; Kawanaka et al., 2004; Bi et al., 2005). The reason for this is the different volatility of PAHs, since more volatile species are absorbed to fine aerosol and are distributed in coarse particles by rapid volatilization and condensation. In comparison, for the PAHs with more rings, due to the lower vapor pressures, the time required for this repartitioning process is much longer (Bi et al., 2005); therefore, they tend to remain in fine particles that are initially emitted (Duan et al., 2007). This hypothesis can explain the relatively higher abundance of more volatile PAHs in the coarse particle mode. Similarly, it can be applied to the size distribution of particle-associated PBDEs. To further confirm this hypothesis, the geometric mass diameter (GMD) for particulate PBDEs was calculated and correlated with logarithmic subcooled liquid vapor pressures ($\log P_L$) (Fig. 4). The mean GMD values for all PBDE congeners ranged from 1.9 to 2.9 μm in Shanghai, which was higher than those in Greece (0.14–0.63 μm) (Mandalakis et al., 2009) and Guangzhou (0.98–1.98 μm) (Luo et al., 2014b). Moreover, there is a positive moderate correlation between GMD and $\log P_L$ ($r = 0.69$, $p < 0.01$), indicating that the GMD increases as the volatile of PBDE congeners increases. This phenomenon becomes more apparent in the coarse size fraction with an increased positive correlation ($r = 0.75$, $p < 0.01$) (right panel in Fig. 4). This result suggests that most coarse-particle-bound PBDEs contain higher volatile species such as tri- and tetra-BDEs. They are derived from the secondary distribution process, i.e.,

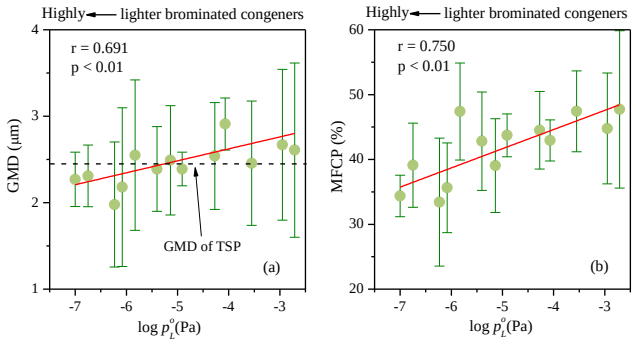

Figure 4. Pearson correlation between GMD and $\log p_{\mathrm{L}}^{\circ}$ of all particulate PBDEs (left) as well as between mass fractions of PBDE congeners in coarse-size particles (MFCP) and $\log p_{\mathrm{L}}^{\circ}$ (right) at 292 K.

revolatilize from fine particles and recondense onto coarse ones (Wang et al., 2008; La Guardia et al., 2006).

Moreover, chemical affinities also played an important role in PBDEs' distribution process. Theoretically, highly brominated congeners have a strong hydrophobicity and prefer to bound with small particles because they have large surface areas (Venkataraman et al., 1999). Such an explanation, however, cannot adequately account for the PBDEs' distribution patterns observed in the present study. Perhaps, in fact, other factors, e.g., emission sources, sampling sites and weather conditions (temperature and/or relative humidity) might also influence their distributions (Zielinska et al., 2004). Although there were still difficulties in totally clarifying the size distributing mechanism of PBDEs or other SVOCs in the current study, it is important to consider integrating all factors in future studies.

3.3 Preliminary study on PBDEs' partitioning mechanisms

Usually, two major mechanisms, i.e., adsorption and absorption, play an important role in PBDEs' partitioning to multimodal urban aerosols (Lohmann and Lammel, 2004). To clarify these processes, the theoretical $K_{\text{p-ads}}$ and $K_{\text{p-abs}}$ were respectively calculated based on Eqs. (3) and (6) because they involved the size-specific parameters, usually including organic matter fractions and the available adsorptive sites, on aerosol particles (Pandis et al., 1992; Pankow, 1994b). The obtained theoretical $K_{\text{p-ads}}$ and $K_{\text{p-abs}}$ values were estimated and compared with measured $K_{\text{p-measured}}$ (from Eq. 7). Since we had no gas PBDEs' concentrations, the measured $K_{\text{p-measured}}$ values were based on a recent study in Shanghai by Yang et al. (2013). In their studies, both gas and particulate PBDEs' concentration were reported at an urban site about ~ 50 km away from our site (Table 1). A range of 10–70 μg m^{-3} was assumed for size-specific particle concentration to calculate $K_{\text{p-measured}}$. The measurement periods ranged from September 2008 to August 2009. The average temperature was 18.4 °C, similar to the temperatures in our study (19 °C). Therefore, their data could serve as a useful reference for us to compare with the theoretical $K_{\text{p-ads}}$ and $K_{\text{p-abs}}$ derived from adsorption and absorption in our study. Note that we took < 0.4, 0.4–2.1 and > 2.1 μm for Aitken, accumulation and coarse mode, respectively.

The plots of measured $\log K_{\text{p-measured}}$ vs. $\log p_{\mathrm{L}}^{\circ}$ and $\log K_{\mathrm{OA}}$ were presented in Fig. 5, along with two sets of theoretical $K_{\text{p-ads}}$ and $K_{\text{p-abs}}$ based on adsorption and absorption in three modes. As presented, significant linear correlations were found between measured $\log K_{\text{p-measured}}$ and $\log p_{\mathrm{L}}^{\circ}$ ($R^2 = 0.76$) as well as measured $\log K_{\text{p-measured}}$ and $\log K_{\mathrm{OA}}$ ($R^2 = 0.77$). For the same class compounds under equilibrium conditions by either adsorption or absorption, the slope of log–log plots of K_{p} and p_{L}° was expected to be close to −1 (Pankow and Bidleman, 1992) and the slope of log–log plots of K_{p} and K_{OA} should be close to 1 (Finizio et al., 1997). However, more gentle regression lines (slopes: −0.53, 0.68) were detected (Fig. 5), similar to slopes reported in previous studies (Cetin and Odabasi, 2008; Yang et al., 2012). The deviations were possibly caused by kinetic limitations (nonequilibrium partition), thermodynamic limitations (lack of constancy in desorption) and additional sorption (Harner and Bidleman, 1998; Cousins and Mackay, 2001; Lohmann et al., 2007).

The three mode data sets of theoretical $\log K_{\text{p-ads}}$ and $\log K_{\text{p-abs}}$ in Fig. 5a and b were calculated using Eqs. (3) and (6), considering only the adsorption mechanism or the absorption mechanism, respectively. As expected, the slopes for them were all −1. Both $\log K_{\text{p-ads}}$ considering only adsorption and $\log K_{\text{p-abs}}$ considering only absorption were compared with measured $\log K_{\text{p-meaused}}$ in Fig. 5. The results showed that the $K_{\text{p-measured}}$ values of highly brominated congeners (e.g., BDE-85, 99, 100, 138, 153, 154 and 183) in three modes fell into the regression line of the theoretical $K_{\text{p-ads}}$. (Fig. 5a), while the measured $K_{\text{p-measured}}$ values of lighter brominated congeners (e.g., BDE-17, 28, 47 and 66) in three modes fell into the regression line of the theoretical $K_{\text{p-abs}}$ (Fig. 5b). These facts revealed that adsorption on surfaces of particles appeared to be responsible for the bimodal distribution of highly brominated congeners, while absorption into organic matter seemed to play an important role for lighter brominated congeners. In addition, we found that the measured $K_{\text{p-measured}}$ lines are both close to the theoretical $K_{\text{p-ads}}$ line in Aitken regression lines (Fig. 5a) and the theoretical $K_{\text{p-abs}}$ lines in the accumulation and coarse regression lines (Fig. 5b). This meant that the mechanisms controlling the particle size distribution of PBDEs included adsorption to Aitken-mode particles and absorption to accumulation- and coarse-mode particles. Adsorption is dependent on available aerosol surface area (A_{TSP}) and absorption on available aerosol organic mass (f_{OM}). Although A_{TSP} and f_{OM} could not be measured and empirical data of A_{TSP} or fOM were adopted from references in this paper, we did provide a way

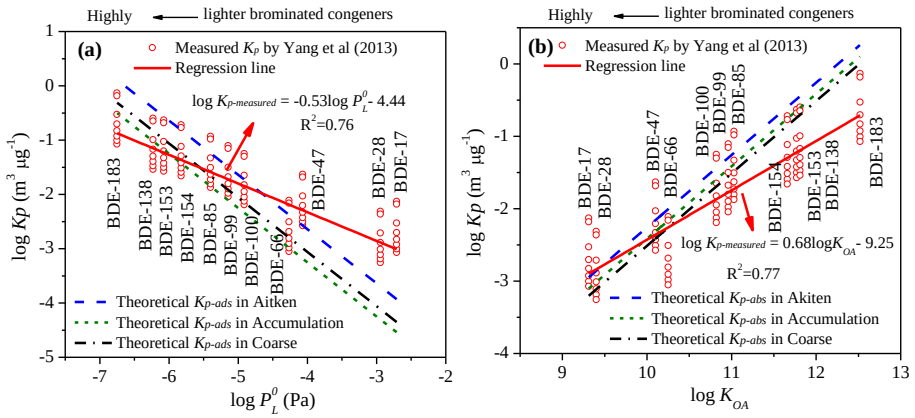

Figure 5. Comparison of theoretical K_p based on adsorption **(a)** and absorption **(b)** in three modes with measured K_p values by Yang et al. (2013) in Shanghai from 2008 to 2009.

Table 4. Pearson correlation matrix for the concentrations of PBDE congeners.

	BDE-17	BDE-28	BDE-71	BDE-47	BDE-66	BDE-100	BDE-99	BDE-85	BDE-154	BDE-153	BDE-138	BDE-183	BDE-190
BDE-17	1	**0.75**[b]	**0.45**[a]	0.18	−0.11	**0.69**[b]	0.18	0.38	−0.11	−0.16	0.11	0.39	0.16
BDE-28		1	**0.65**[b]	−0.05	0.39	**0.69**[b]	**0.45**[a]	**0.69**[b]	−0.16	0.05	0.04	0.28	0.15
BDE-71			1	0.16	0.27	**0.82**[b]	**0.60**[b]	**0.70**[b]	−0.06	0.34	0.31	0.18	**0.48**[a]
BDE-47				1	0.01	0.36	−0.22	−0.19	0.08	−0.27	−0.08	0.24	**0.71**[b]
BDE-66					1	0.27	0.30	**0.51**[a]	0.26	0.18	−0.10	−0.06	0.25
BDE-100						1	**0.54**[a]	**0.67**[b]	0.11	0.13	0.22	0.19	**0.57**[b]
BDE-99							1	**0.83**[b]	0.14	0.37	**0.68**[b]	0.30	0.41
BDE-85								1	0.18	0.37	**0.44**[a]	0.21	0.37
BDE-154									1	0.35	0.34	0.20	0.19
BDE-153										1	**0.56**[b]	−0.07	0.09
BDE-138											1	**0.47**[a]	0.37
BDE-183												1	0.28
BDE-190													1

Significant values are marked in bold. [a] Correlation is significant at 0.05 level (two-tailed). [b] Correlation is significant at 0.01 level (two-tailed).

to investigate the mechanisms for size distribution of SVOCs from the view of gas–particle partition.

3.4 Correlation analysis of PBDEs

Table 4 presents a Pearson correlation matrix among PBDE congeners based on concentrations. Significant correlation was found among the tri-BDEs (BDE-17 and 28, $r = 0.75$, $p<0.05$), as well as penta-BDEs (BDE-100, 99 and 85, $r = 0.67$–0.83, $p<0.05$). These high-correlation values suggested that tri-BDEs and/or penta-BDEs shared a common source and/or exhibited a similar distribution behavior in environment. BDE-28 significantly correlated with BDE-71 ($r = 0.65$, $p<0.05$), and both of them also significantly correlated with penta-BDEs 100, 99 and 85. As we know, penta-BDEs were frequently detected in ambient particles around solid waste incineration plants (Dong et al., 2015). In this observation, we also found that penta-BDEs appeared in high concentrations (mean: 49.5 pg m^{-3}) compared with other congeners. Thus, we concluded that these penta-BDEs and correlated congeners probably came from the same source regions because there are numerous solid waste incineration plants located in surrounding places of Shanghai. Hepta-BDE (BDE-183 and 190) correlated poorly with the other congeners, with only two exceptions, which were statistically significant at the $r = 0.47$, $p<0.01$ level for BDE-183 and 138, as well as $r = 0.71$, $p<0.05$ level for BDE-190 and 47, respectively. This suggested that hepta-BDEs might not originate from the same sources. Other studies showed the possibility of the decomposition of higher brominated PBDEs to form lower brominated PBDEs in the atmosphere (Eriksson et al., 2004; Söderström et al., 2004; Kajiwara et al., 2008). Here we did not measure higher brominated PBDEs (octa- and deca-BDEs) and no correlation analysis was performed on them. However, as seen in Fig. 1, the hexa- versus hepta-BDEs concentrations (mean: 16.7 and 11.2 pg m^{-3}) were relatively high, and thus indicative of multiple releasing sources in this area; i.e., local emissions, higher brominated PBDEs breakdown and long-range atmospheric transport may have potentially contributed to hexa- and hepta-BDEs' contaminations.

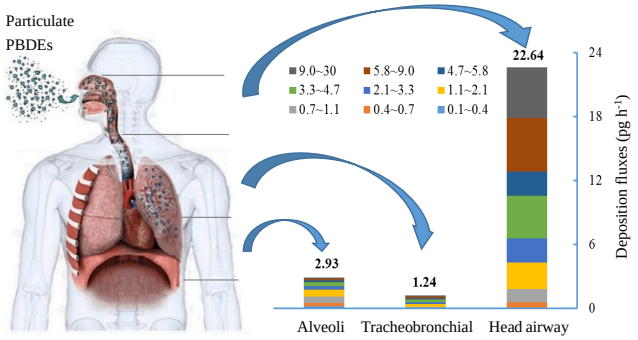

Figure 6. Deposition fluxes of size-resolved particulate PBDEs in the human respiratory tract.

3.5 Implications for health

In this section, we calculated the regional deposition flux in the human respiratory tract based on Eqs. (8), (9) and (10). Figure 6 showed the deposition fluxes of size-resolved PBDEs for adult men. The total deposition fluxes of Σ13 PBDEs were calculated at 26.8 pg h^{-1}. Among these compounds, penta-BDEs were the major congeners and contributed a mean value of 58 % (range: 31–70 %) to the total deposition fluxes. The percent contribution of Σ13 PBDEs to the respiratory tract was 84.4 % (22.64 ng h^{-1}) in the head airway, 4.6 % (1.24 ng h^{-1}) in the tracheobronchial and 11.0 % (2.93 pg h^{-1}) in the alveoli regions, respectively. Moreover, we also found that coarse particles contributed major PBDEs in the head and tracheobronchial regions, while fine particles (accumulation- plus Aitken-mode particles) contributed many PBDEs in the alveoli region. As we know, the size distribution of particle-associated PBDEs has a decisive influence on their potential health effects. Considering that fine particles can penetrate deeper into the respiratory system compared to coarse particles, fine-particle-bound PBDEs are expected to accumulate in the lower parts of the lungs and pose a greater risk to human health.

We further evaluated the human health risk that is caused by PBDEs by using a HQ approach based on data on inhaled PBDEs. Fig. 7 showed that the HQ values of the individual congeners ranged from 4.0×10^{-7} to 6.8×10^{-5}, with a total value of 1.6×10^{-4} for Σ13 PBDEs. During the assessment process, we found that the HQ values were highly dependent on the variable daily intake (DI, see Eq. 12), which was inconstant and would result in uncertainty in the risk evaluation. Taking these situations into consideration, we utilized Monte Carlo (MC) simulation to evaluate the influences of uncertainty on this exposure model and to examine whether a difference exists between the model and the calculated HQ. In the simulation, the MC procedure was repeated 5000 times with different calculated HQ values. The results of the simulation are depicted in Fig. 8, which exhibits a wide gamma distribution. The 95 % percentile val-

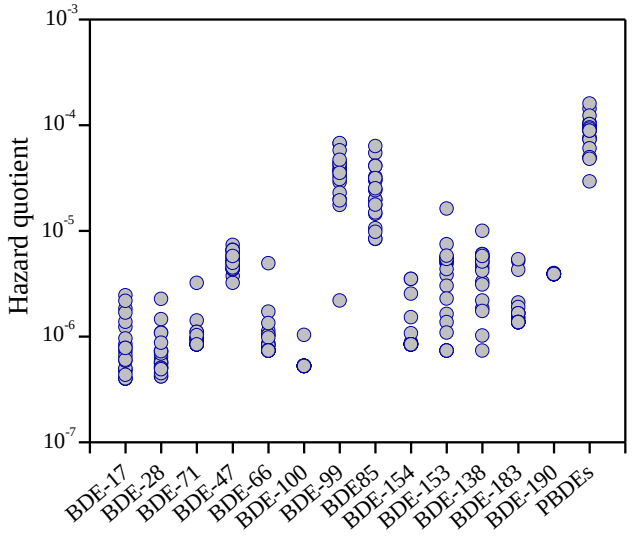

Figure 7. Hazard quotient (HQ) for particulate PBDEs in the atmosphere of Shanghai. PBDEs are the sum of BDE-17, 28, 71, 47, 66, 100, 99, 85, 154, 153, 138, 183, and 190.

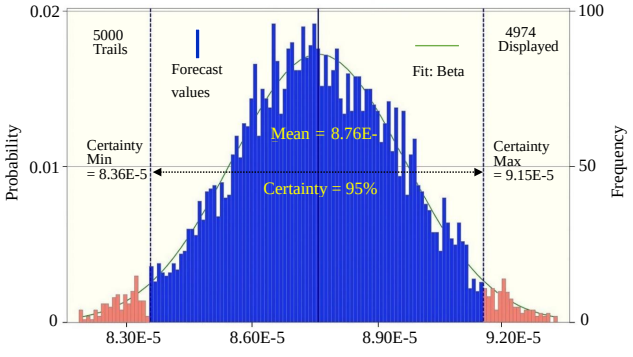

Figure 8. Probability distributions of hazard quotient of PBDEs in Monte Carlo simulations with 5000 trials.

ues of HQ were in the range 9.15–8.36 × 10^{-5}, with a mean value of 8.76×10^{-5}. In comparison with the corresponding experimental HQ data (1.6×10^{-4}), excellent agreement could be observed between the data, indicating the accuracy of our simulation. By comparison, these HQ values in the present study were much lower than the risk guideline value (1.0) recommended by the US Environmental Protection Agency. Even under heavy exercise conditions (assuming a high breathing rate of 3 m^3 h^{-1}), the estimated HQ of Σ13 PBDEs was only $(1.17 \pm 0.42) \times 10^{-3}$, far less than 1. Thus, particulate PBDEs in the atmosphere of the urban site of Shanghai posed low non-cancer risk through inhalation. However, it was noteworthy here that only particle-phase PBDEs were included in the assessment and we were not sure whether the risk posed by atmospheric PBDEs (gas plus particles) exceeded the threshold. Specifically, BDE-47 and BDE-99 mainly existed in the gas phase, and were

probably more toxic and bioaccumulative than other congeners (Darnerud, 2003). Furthermore, we only measured 13 PBDE congeners, neglecting risk caused by substantial octa-BDE and deca-BDE in particles, and other types of exposure, like ingestion or dermal contact, were not considered either. Thus, it can not be suggested that the occurrence of particulate PBDEs in Shanghai is not an issue; rather, we advocate further studies that measure more PBDE congeners in not only particle phase, but also gas phase, in relation to health risk assessment.

4 Summary and conclusions

This study revealed the size distribution of particle-associated PBDEs in the urban atmosphere of Shanghai and calculated the contribution of each size-specific particle to PBDEs deposited in the respiratory tract. The particle size distribution of PBDEs was a bimodal distribution with one peak at fine size fractions and the second peak at coarse size fractions. The peaks' intensities were associated the molecular weights of PBDEs. The possible reasons were expounded by the parameters such as physicochemical properties of PBDEs, meteorological factors and the emission source. Adsorption and absorption mechanisms played crucial roles in highly and lightly brominated congeners, respectively. Most PBDEs were predominantly distributed in small particles, which contributed the majority of PBDEs' deposition fluxes in the human respiratory tract. Total deposition fluxes of target $\Sigma 13$ PBDEs in the respiratory tract was calculated to be $26.8\,\mathrm{ng\,h^{-1}}$. The non-cancer risk of PBDEs from inhaling particles in the urban atmosphere of Shanghai was shown to be somewhat low. Further studies will be focused on the investigations of fine or ultrafine particles as transporters of toxic compounds from the atmosphere to the respiratory tract, and the evaluation of exposure risks of ultrafine particles in the atmosphere.

Acknowledgements. This work was supported by the National Natural Science Foundation of China (nos. 21577021, 21177025, 21377028, 21277082, 41475109), the Excellent Academic Leader Program (no. 14XD1400600), the National Key Technology R&D Program of Ministry of Science and Technology (2014BAC16B01), FP720 project (AMIS, IRSES-GA-2011) and the program for New Century Excellent Talents in University (NCET-13-0349).

Edited by: F. Pope

References

Alaee, M., Arias, P., Sjodin, A., and Bergman, A.: An overview of commercially used brominated flame retardants, their applications, their use patterns in different countries/regions and possible modes of release, Environ. Int., 29, 683–689, 2003.

Aubin, D. G. and Abbatt, J. P.: Laboratory measurements of thermodynamics of adsorption of small aromatic gases to *n*-hexane soot surfaces, Environ. Sci. Technol., 40, 179–187, 2006.

Besis, A. and Samara, C.: Polybrominated diphenyl ethers (PBDEs) in the indoor and outdoor environments – a review on occurrence and human exposure, Environ. Pollut., 169, 217–229, 2012.

Besis, A., Botsaropoulou, E., Voutsa, D., and Samara, C.: Particle-size distribution of polybrominated diphenyl ethers (PBDEs) in the urban agglomeration of Thessaloniki, northern Greece, Atmos. Environ., 104, 176–185, 2015.

Betts, K. S.: Unwelcome guest: PBDEs in indoor dust, Environ. Health Perspect., 116, A202–A208, 2008.

Bezares-Cruz, J., Jafvert, C. T., and Hua, I.: Solar photodecomposition of decabromodiphenyl ether: products and quantum yield, Environ. Sci. Technol., 38, 4149–4156, 2004.

Bi, X., Sheng, G., Peng, P. A., Chen, Y., and Fu, J.: Size distribution of *n*-alkanes and polycyclic aromatic hydrocarbons (PAHs) in urban and rural atmospheres of Guangzhou, China, Atmos. Environ., 39, 477–487, 2005.

Castro-Jimenez, J., Mariani, G., Vives, I., Skejo, H., Umlauf, G., Zaldivar, J. M., Dueri, S., Messiaen, G., and Laugier, T.: Atmospheric concentrations, occurrence and deposition of persistent organic pollutants (POPs) in a Mediterranean coastal site (Etang de Thau, France), Environ. Pollut., 159, 1948–1956, 2011.

Cetin, B. and Odabasi, M.: Atmospheric concentrations and phase partitioning of polybrominated diphenyl ethers (PBDEs) in Izmir, Turkey, Chemosphere, 71, 1067–1078, 2008.

Cousins, I. T. and Mackay, D.: Gas–particle partitioning of organic compounds and its interpretation using relative solubilities, Environ. Sci. Technol., 35, 643–647, 2001.

Darnerud, P. O.: Toxic effects of brominated flame retardants in man and in wildlife, Environ. Int., 29, 841–853, 2003.

de Wit, C. A.: An overview of brominated flame retardants in the environment, Chemosphere, 46, 583–624, 2002.

Dong, Y., Fu, S., Zhang, Y., Nie, H., and Li, Z.: Polybrominated diphenyl ethers in atmosphere from three different typical industrial areas in Beijing, China, Chemosphere, 123, 33–42, 2015.

Duan, J. C., Bi, X. H., Tan, J. H., Sheng, G. Y., and Fu, J. M.: Seasonal variation on size distribution and concentration of PAHs in Guangzhou city, China, Chemosphere, 67, 614–622, 2007.

Eriksson, J., Green, N., Marsh, G., and Bergman, A.: Photochemical decomposition of 15 polybrominated diphenyl ether congeners in methanol/water, Environ. Sci. Technol., 38, 3119–3125, 2004.

Finizio, A., Mackay, D., Bidleman, T., and Harner, T.: Octanol-air partition coefficient as a predictor of partitioning of semi-volatile organic chemicals to aerosols, Atmos. Environ., 31, 2289–2296, 1997.

Geiser, M., Rothen-Rutishauser, B., Kapp, N., Schurch, S., Kreyling, W., Schulz, H., Semmler, M., Hof, V. I., Heyder, J., and Gehr, P.: Ultrafine particles cross cellular membranes by non-phagocytic mechanisms in lungs and in cultured cells, Environ. Health Perspect., 113, 1555–1560, 2005.

Hale, R. C., Alaee, M., Manchester-Neesvig, J. B., Stapleton, H. M., and Ikonomou, M. G.: Polybrominated diphenyl ether flame re-

tardants in the North American environment, Environ. Int., 29, 771–779, 2003.

Harner, T. and Bidleman, T. F.: Octanol-air partition coefficient for describing particle/gas partitioning of aromatic compounds in urban air, Environ. Sci. Technol., 32, 1494–1502, 1998.

Harner, T. and Shoeib, M.: Measurements of octanol-air partition coefficients (K-OA) for polybrominated diphenyl ethers (PBDEs): predicting partitioning in the environment, J. Chem. Eng. Data, 47, 228–232, 2002.

Harrad, S., de Wit, C. A., Abdallah, M. A.-E., Bergh, C., Björklund, J. A., Covaci, A., Darnerud, P. O., de Boer, J., Diamond, M., and Huber, S.: Indoor contamination with hexabromocyclododecanes, polybrominated diphenyl ethers, and perfluoroalkyl compounds: an important exposure pathway for people?, Environ. Sci. Technol., 44, 3221–3231, 2010.

Hoh, E. and Hites, R. A.: Brominated flame retardants in the atmosphere of the East-Central United States, Environ. Sci. Technol., 39, 7794–7802, 2005.

International Commission on Radiological Protection, I.: ICRP Publication 66: Human Respiratory Tract Model for Radiological Protection, 66, Elsevier Health Sciences, New York, USA, 1995.

Kajiwara, N., Noma, Y., and Takigami, H.: Photolysis studies of technical decabromodiphenyl ether (DecaBDE) and ethane (DeBDethane) in plastics under natural sunlight, Environ. Sci. Technol., 42, 4404–4409, 2008.

Kakimoto, K., Nagayoshi, H., Takagi, S., Akutsu, K., Konishi, Y., Kajimura, K., Hayakawa, K., and Toriba, A.: Inhalation and dietary exposure to Dechlorane Plus and polybrominated diphenyl ethers in Osaka, Japan, Ecotoxicol. Environ. Saf., 99, 69–73, 2014.

Kavouras, I. G., Lawrence, J., Koutrakis, P., Stephanou, E. G., and Oyola, P.: Measurement of particulate aliphatic and polynuclear aromatic hydrocarbons in Santiago de Chile: source reconciliation and evaluation of sampling artifacts, Atmos. Environ., 33, 4977–4986, 1999.

Kawanaka, Y., Matsumoto, E., Sakamoto, K., Wang, N., and Yun, S. J.: Size distributions of mutagenic compounds and mutagenicity in atmospheric particulate matter collected with a low-pressure cascade impactor, Atmos. Environ., 38, 2125–2132, 2004.

Kemmlein, S., Herzke, D., and Law, R. J.: Brominated flame retardants in the European chemicals policy of REACH – regulation and determination in materials, J. Chromatogr. A, 1216, 320–333, 2009.

La Guardia, M. J., Hale, R. C., and Harvey, E.: Detailed polybrominated diphenyl ether (PBDE) congener composition of the widely used penta-, octa-, and deca-PBDE technical flame-retardant mixtures, Environ. Sci. Technol., 40, 6247–6254, 2006.

Larsen, R. K. and Baker, J. E.: Source apportionment of polycyclic aromatic hydrocarbons in the urban atmosphere: a comparison of three methods, Environ. Sci. Technol., 37, 1873–1881, 2003.

Lee, R. G. M., Thomas, G. O., and Jones, K. C.: PBDEs in the atmosphere of three locations in Western Europe, Environ. Sci. Technol., 38, 699–706, 2004.

Li, P. F., Li, X., Yang, C. Y., Wang, X. J., Chen, J. M., and Collett, J. L.: Fog water chemistry in Shanghai, Atmos. Environ., 45, 4034–4041, 2011.

Li, X., Li, P., Yan, L., Chen, J., Cheng, T., and Xu, S.: Characterization of polycyclic aromatic hydrocarbons in fog-rain events, J. Environ. Monit., 13, 2988–2993, 2011.

Li, Y., Lin, T., Wang, F., Ji, T., and Guo, Z.: Seasonal variation of polybrominated diphenyl ethers in $PM_{2.5}$ aerosols over the East China Sea, Chemosphere, 119, 675–681, 2015.

Lohmann, R. and Lammel, G.: Adsorptive and absorptive contributions to the gas-particle partitioning of polycyclic aromatic hydrocarbons: state of knowledge and recommended parametrization for modeling, Environ. Sci. Technol., 38, 3793–3803, 2004.

Lohmann, R., Gioia, R., Eisenreich, S. J., and Jones, K. C.: Assessing the importance of ab- and adsorption to the gas-particle partitioning of PCDD/Fs, Atmos. Environ., 41, 7767–7777, 2007.

Luo, P., Bao, L.-J., Wu, F.-C., Li, S.-M., and Zeng, E. Y.: Health risk characterization for resident inhalation exposure to particle-bound halogenated flame retardants in a typical E-waste recycling zone, Environ. Sci. Technol., 48, 8815–8822, 2014a.

Luo, P., Ni, H. G., Bao, L. J., Li, S. M., and Zeng, E. Y.: Size distribution of airborne particle-bound polybrominated diphenyl ethers and its implications for dry and wet deposition, Environ. Sci. Technol., 48, 13793–13799, 2014b.

Lv, Y., Li, X., Xu, T. T., Cheng, T. T., Yang, X., Chen, J. M., Linuma, Y., and Herrmann, H.: Size distributions of polycyclic aromatic hydrocarbons in urban atmosphere: sorption mechanism and source contributions to respiratory deposition, Atmos. Chem. Phys. Discuss., 15, 20811–20850, doi:10.5194/acpd-15-20811-2015, 2015.

Mandalakis, M., Besis, A., and Stephanou, E. G.: Particle-size distribution and gas/particle partitioning of atmospheric polybrominated diphenyl ethers in urban areas of Greece, Environ. Pollut., 157, 1227–1233, 2009.

Marklund, A., Andersson, B., and Haglund, P.: Screening of organophosphorus compounds and their distribution in various indoor environments, Chemosphere, 53, 1137–1146, 2003.

Moller, A., Xie, Z. Y., Cai, M. H., Zhong, G. C., Huang, P., Cai, M. G., Sturm, R., He, J. F., and Ebinghaus, R.: Polybrominated diphenyl ethers vs. alternate brominated flame retardants and dechloranes from East Asia to the Arctic, Environ. Sci. Technol., 45, 6793–6799, 2011.

Muenhor, D., Harrad, S., Ali, N., and Covaci, A.: Brominated flame retardants (BFRs) in air and dust from electronic waste storage facilities in Thailand, Environ. Int., 36, 690–698, 2010.

Okonski, K., Degrendele, C., Melymuk, L., Landlova, L., Kukucka, P., Vojta, S., Kohoutek, J., Cupr, P., and Klanova, J.: Particle size distribution of halogenated flame retardants and implications for atmospheric deposition and transport, Environ. Sci. Technol., 48, 14426–14434, 2014.

Pandis, S. N., Harley, R. A., Cass, G. R., and Seinfeld, J. H.: Secondary organic aerosol formation and transport, Atmos. Environ., 26, 2269–2282, 1992.

Pankow, J. F.: Review and comparative-analysis of the theories on partitioning between the gas and aerosol particulate phases in the atmosphere, Atmos. Environ., 21, 2275–2283, 1987.

Pankow, J. F.: An absorption-model of gas-particle partitioning of arganic-compounds in the atmosphere, Atmos. Environ., 28, 185–188, 1994a.

Pankow, J. F.: An absorption-model of the gas aerosol partitioning involved in the formation of secondary organic aerosol, Atmos. Environ., 28, 189–193, 1994b.

Pankow, J. F. and Bidleman, T. F.: Interdependence of the slopes and intercepts from log log correlations of measured gas particle partitioning and vapor-pressure.1.Theory and analysis of available data, Atmos. Environ., 26, 1071–1080, 1992.

Rudich, Y., Donahue, N. M., and Mentel, T. F.: Aging of organic aerosol: bridging the gap between laboratory and field studies, Annu. Rev. Phys. Chem., 58, 321–352, 2007.

Söderström, G., Sellström, U., de Wit, C. A., and Tysklind, M.: Photolytic debromination of decabromodiphenyl ether (BDE 209), Environ. Sci. Technol., 38, 127–132, 2004.

Shen, X., Zhao, Y., Chen, Z., and Huang, D.: Heterogeneous reactions of volatile organic compounds in the atmosphere, Atmos. Environ., 68, 297–314, 2013.

Shi, J. and Cui, L. L.: Characteristics of high impact weather and meteorological disaster in Shanghai, China, Nat. Hazards, 60, 951–969, 2012.

Su, Y. S., Hung, H., Brice, K. A., Su, K., Alexandrou, N., Blanchard, P., Chan, E., Sverko, E., and Fellin, P.: Air concentrations of polybrominated diphenyl ethers (PBDEs) in 2002–2004 at a rural site in the Great Lakes, Atmos. Environ., 43, 6230–6237, 2009.

Tian, M., Chen, S.-J., Wang, J., Zheng, X.-B., Luo, X.-J., and Mai, B.-X.: Brominated flame retardants in the atmosphere of E-waste and rural sites in Southern China: seasonal variation, temperature dependence, and gas-particle partitioning, Environ. Sci. Technol., 45, 8819–8825, 2011.

Tittlemier, S. A., Halldorson, T., Stern, G. A., and Tomy, G. T.: Vapor pressures, aqueous solubilities, and Henry's law constants of some brominated flame retardants, Environ. Toxicol. Chem., 21, 1804–1810, 2002.

Venkataraman, C., Thomas, S., and Kulkarni, P.: Size distributions of polycyclic aromatic hydrocarbons – gas/particle partitioning to urban aerosols, J. Aerosol Sci., 30, 759–770, 1999.

Volckens, J. and Leith, D.: Effects of sampling bias on gas–particle partitioning of semi-volatile compounds, Atmos. Environ., 37, 3385–3393, 2003.

Wang, J., Ho, S. S. H., Cao, J., Huang, R., Zhou, J., Zhao, Y., Xu, H., Liu, S., Wang, G., Shen, Z., and Han, Y.: Characteristics and major sources of carbonaceous aerosols in $PM_{2.5}$ from Sanya, China, Sci. Total Environ., 530–531, 110–119, 2015.

Wang, X. M., Ding, X., Mai, B. X., Xie, Z. Q., Xiang, C. H., Sun, L. G., Sheng, G. Y., Fu, J. M., and Zeng, E. Y.: Polyhrominated diphenyl ethers in airborne particulates collected during a research expedition from the Bohai Sea to the Arctic, Environ. Sci. Technol., 39, 7803–7809, 2005.

Wang, Z.-Y., Zeng, X.-L., and Zhai, Z.-C.: Prediction of supercooled liquid vapor pressures and n-octanol/air partition coefficients for polybrominated diphenyl ethers by means of molecular descriptors from DFT method, Sci. Total Environ., 389, 296–305, 2008.

Wensing, M., Uhde, E., and Salthammer, T.: Plastics additives in the indoor environment – flame retardants and plasticizers, Sci. Total Environ., 339, 19–40, 2005.

Wilford, B. H., Harner, T., Zhu, J. P., Shoeib, M., and Jones, K. C.: Passive sampling survey of polybrominated diphenyl ether flame retardants in indoor and outdoor air in Ottawa, Canada: implications for sources and exposure, Environ. Sci. Technol., 38, 5312–5318, 2004.

Yang, M., Jia, H. L., Ma, W. L., Qi, H., Cui, S., and Li, Y. F.: Levels, compositions, and gas-particle partitioning of polybrominated diphenyl ethers and dechlorane plus in air in a Chinese northeastern city, Atmos. Environ., 55, 73–79, 2012.

Yang, M., Qi, H., Jia, H. L., Ren, N. Q., Ding, Y. S., Ma, W. L., Liu, L. Y., Hung, H., Sverko, E., and Li, Y. F.: Polybrominated diphenyl ethers in air across China: levels, compositions, and gas-particle partitioning, Environ. Sci. Technol., 47, 8978–8984, 2013.

Yu, H. and Yu, J. Z.: Polycyclic aromatic hydrocarbons in urban atmosphere of Guangzhou, China: size distribution characteristics and size-resolved gas-particle partitioning, Atmos. Environ., 54, 194–200, 2012.

Yu, Z., Liao, R., Li, H., Mo, L., Zeng, X., Sheng, G., and Fu, J.: Particle-bound Dechlorane Plus and polybrominated diphenyl ethers in ambient air around Shanghai, China, Environ. Pollut., 159, 2982–2988, 2011.

Zhang, B. Z., Guan, Y. F., Li, S. M., and Zeng, E. Y.: Occurrence of Polybrominated Diphenyl Ethers in Air and Precipitation of the Pearl River Delta, South China: annual Washout Ratios and Depositional Rates, Environ. Sci. Technol., 43, 9142–9147, 2009.

Zhang, B. Z., Zhang, K., Li, S. M., Wong, C. S., and Zeng, E. Y.: Size-dependent dry deposition of airborne polybrominated diphenyl ethers in urban Guangzhou, China, Environ. Sci. Technol., 46, 7207–7214, 2012.

Zhang, K., Zhang, B. Z., Li, S. M., Wong, C. S., and Zeng, E. Y.: Calculated respiratory exposure to indoor size-fractioned polycyclic aromatic hydrocarbons in an urban environment, Sci. Total Environ., 431, 245–251, 2012.

Zielinska, B., Sagebiel, J., Arnott, W. P., Rogers, C. F., Kelly, K. E., Wagner, D. A., Lighty, J. S., Sarofim, A. F., and Palmer, G.: Phase and size distribution of polycyclic aromatic hydrocarbons in diesel and gasoline vehicle emissions, Environ. Sci. Technol., 38, 2557–2567, 2004.